

# Heavy-fermions in frustrated Hund's metal with portions of incipient flat-bands

Yilin Wang<sup>1,2,3,\*</sup>

<sup>1</sup>Hefei National Research Center for Interdisciplinary Sciences at the Microscale,  
University of Science and Technology of China, Hefei 230026, China

<sup>2</sup>Hefei National Laboratory, University of Science and Technology of China, Hefei 230088, China

<sup>3</sup>New Cornerstone Science Laboratory, University of Science and Technology of China, Hefei, 230026, China

(Dated: January 31, 2024)

Flat-bands induced by destructive interference of hoppings in frustrated lattices such as kagome metals, have been extensively studied in recent years since they may lead to strongly correlated phenomena. However, in realistic multiorbital  $d$ -electron materials, such flat-bands usually appear in small portions of Brillouin zone and are away from Fermi level (dubbed as “incipient”). Whether such incipient flat-band portions can induce very strong electron correlations is an open question. Here, by density functional theory plus dynamical mean-field theory calculations on the superconducting kagome  $\text{CsCr}_3\text{Sb}_5$  and triangular  $\text{CrB}_2$ , we show that the roles of such incipient flat-bands in driving electron correlations can be significantly amplified by Hund's coupling  $J_H$  in a Hund's metal. As a result, even moderately  $d$ -electron heavy-fermions could be induced by enhancing the orbital differentiation and Kondo-like effect of Hund's metals. This provides a flexible route for generating  $d$ -electron heavy-fermion, and for controllably inducing electron correlations and magnetic fluctuations suitable for emergence of unconventional superconductivity, in frustrated Hund's metals with portions of incipient flat-bands.

*Introduction.* In narrow/flat band systems, electron-electron interaction usually give rise to strongly correlated phenomena [1–7]. For example, heavy-fermions are induced via Kondo effect in  $f$ -electron systems with extremely flat  $f$ -bands at Fermi level ( $E_F$ ) [8–10]. Flat-bands could be also induced in frustrated lattices by destructive interference of hoppings [11–14], such as those extensively studied in kagome metals [15–24]. However, in multiorbital  $d$ -electron materials, such flat-bands usually appear in small portions of Brillouin zone (BZ) and are away from  $E_F$  (dubbed as incipient flat bands [25]). Whether such incipient flat-band portions can induce very strong electron correlations and even heavy-fermions is an open question.

In multiorbital  $d$ -electron systems, there is one class of strongly correlated metals dubbed as Hund's metals, where correlations mainly derive from Hund's coupling  $J_H$ , not Hubbard  $U$  [26–42]. They usually appear when the electron filling is one-electron away from half-filling [28]. Canonical Hund's metals include iron-based superconductors (6 electrons/5  $d$ -orbitals) [29, 43–45] and  $\text{Sr}_2\text{RuO}_4$  (4 electrons/3  $t_{2g}$  orbitals) [46–50]. Hund's metals show strong orbital differentiation [51–60], i.e., some orbitals are more correlated than the others if they have smaller bandwidths, or just contribute a higher density of states (DOS) at  $E_F$ . Such differentiation in correlations could be significantly amplified via larger  $J_H$  even though the original orbital difference is not that large, which leads to coexistence of heavy and light electrons. Hund's coupling tends to form large local moments which leads to strong incoherence of electrons at high temperature. With decreasing temperature, Hund's metal undergoes a Kondo-like incoherence-to-coherence crossover by screening the local moments, and a renormalized Fermi liquid with large quasi-particle mass emerges at very low

temperature [27, 33, 43, 46, 61, 62]. In this sense, the Hund's metal physics is in the same spirit of Kondo effect. A question thus arises: whether the presence of incipient flat-band portions in a Hund's metal will significantly enhance its orbital differentiation and Kondo-like effect such that heavy-fermions are induced?

In this work, we demonstrate the answer is yes, by performing density functional theory plus dynamical mean-field theory (DFT+DMFT) [63–65] calculations on the superconducting  $\text{CsCr}_3\text{Sb}_5$  and  $\text{CrB}_2$  with frustrated kagome and triangular lattices, respectively.  $\text{CsCr}_3\text{Sb}_5$  is a new  $\text{CsV}_3\text{Sb}_5$ -type [66, 67] kagome superconductor discovered recently [68]. At ambient pressure, the resistivity of  $\text{CsCr}_3\text{Sb}_5$  and  $\text{CrB}_2$  show semiconducting [68] and sublinear [69] behaviors, respectively, indicating bad metals.  $\text{CsCr}_3\text{Sb}_5$  undergoes a charge density wave (CDW) transition and then an anti-ferromagnetic (AFM) transition at low temperature ( $\sim 54$  K) [68]. First-principle calculations suggest it is an altermagnet [70].  $\text{CrB}_2$  undergoes an AFM transition at 88 K [69]. Large specific-heat coefficient  $\gamma \sim 120$  and  $70$   $\text{mJ mol}^{-1} \text{K}^{-2}$  are found for  $\text{CsCr}_3\text{Sb}_5$  and  $\text{CrB}_2$ , respectively, indicating possible moderately heavy-fermions [68, 69]. Under high pressure, the CDW and AFM orders are suppressed and superconductivity occur in both compounds [68, 71, 72].

Our calculations show that both compounds are typical Hund's metals with unusually large quasi-particle mass-enhancement  $m^*/m^{\text{DFT}}$  ( $10 \sim 20$ ), which explains the experimental observations of heavy-fermions. We show that the emergence of heavy-fermions is attributed to the existence of incipient flat-band portions with  $d$ -orbital characters which enhance the orbital differentiation and Kondo-like effect via Hund's coupling  $J_H$ , not Hubbard  $U$ . The electron correlations and magnetism can thus be controlled by tuning the positions and band-

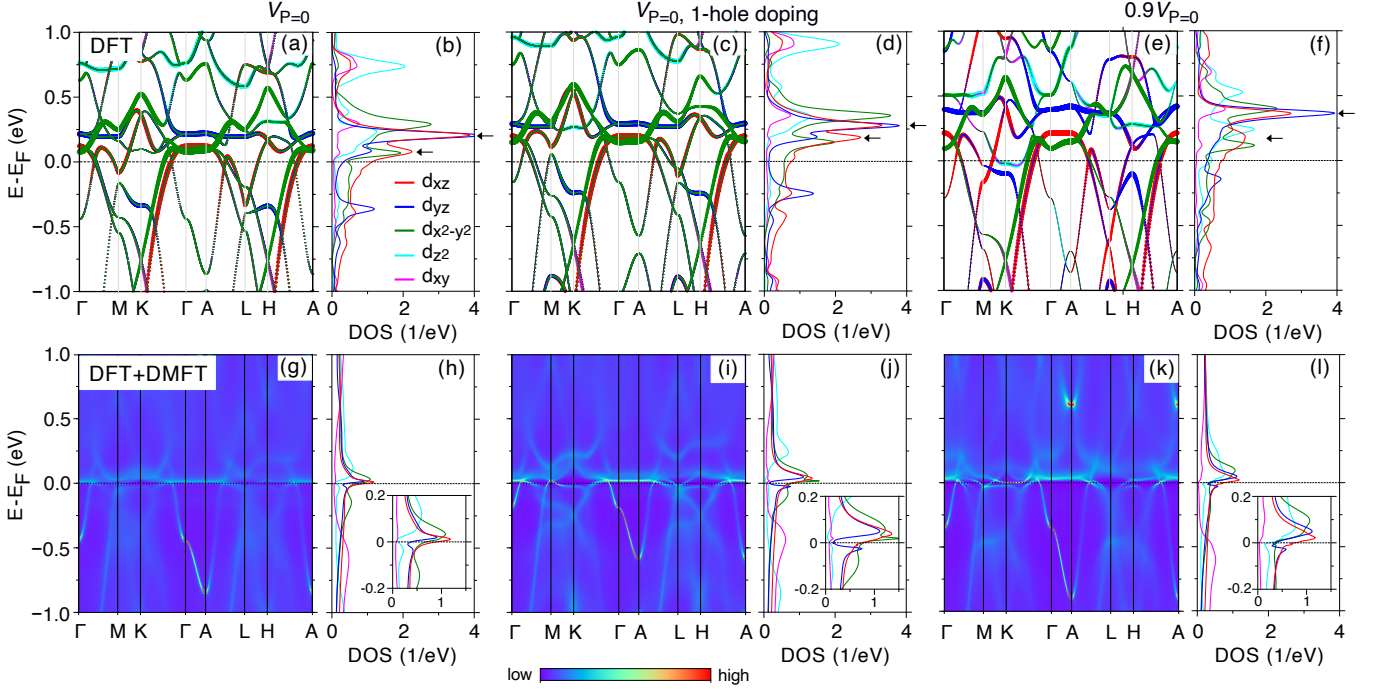


FIG. 1. Incipient flat-bands in  $\text{CsCr}_3\text{Sb}_5$ . (a)-(f) DFT calculated band structures and density of states. (g)-(l) DFT+DMFT calculated spectra functions at  $U = 5$  eV,  $J_H = 0.88$  eV and  $T = 100$  K. (a),(b),(g),(h) Results for ambient pressure with experimental lattice volume  $V_{P=0}$ . (c),(d),(i),(j) Results for ambient pressure, but with one-hole doping. (e),(f),(k),(l) Results for high pressure with  $0.9V_{P=0}$ . The black arrows in (b),(d),(f) indicate the positions of the incipient flat-bands with  $d_{xz}$ ,  $d_{yz}$  and  $d_{x^2-y^2}$  characters, which are pushed further away from  $E_F$  by one-hole doping or high pressure. The insets in (h),(j),(l) are the enlarged density of states from  $-0.2$  to  $0.2$  eV.

widths of these incipient flat-bands via carrier doping or pressure. This provides a flexible route for generating  $d$ -electron heavy-fermions, and for controllably inducing electron correlations and magnetic fluctuations suitable for emergence of unconventional superconductivity, in frustrated Hund's metals with portions of incipient flat-bands.

*Methods.* Fully charge self-consistent single-site DFT+DMFT calculations are performed for the paramagnetic phases of  $\text{CsCr}_3\text{Sb}_5$  and  $\text{CrB}_2$ , using the DFT+eDMFT code developed by Haule *et al.* [73, 74] based on the WIEN2K package [75]. A large hybridization energy window from  $-10$  to  $10$  eV is included. All five  $d$ -orbitals are considered as correlated ones, and an “exact” double-counting scheme is chosen [76]. The continuous time quantum Monte Carlo [77] is used as impurity solver. The self-energy on real frequency is obtained by the analytical continuation method of maximum entropy. For  $\text{CsCr}_3\text{Sb}_5$ , we use the experimental lattice constants with a volume of  $V_{P=0}$  at ambient pressure [68], and simulate a high pressure by reducing the volume to  $0.9V_{P=0}$ , since the lattice parameters under high pressure have not been reported experimentally. We simulate a uniform hole-doping by reducing the total valence electrons by one (per unit cell) and compensating it by an uniform

background of positive charges. For  $\text{CrB}_2$ , experimental lattice constants at  $P=0$ , 20 GPa are used [71]. More computational details are presented in the Supplementary Materials [78].

*Heavy fermion in  $\text{CsCr}_3\text{Sb}_5$ .* The DFT calculated band structure and DOS of  $\text{CsCr}_3\text{Sb}_5$  at ambient pressure is shown in Fig. 1(a) and (b). The fat-bands with Cr  $d$ -orbital characters are shown by colors in terms of the point-group of Cr-site ( $D_{2h}$ ). We indeed find portions of incipient flat-bands with  $d_{xz}$  ( $B_{2g}$ , red),  $d_{yz}$  ( $B_{3g}$ , blue),  $d_{x^2-y^2}$  ( $A_g$ , green) characters, which are  $0.1 \sim 0.3$  eV above  $E_F$ . These three orbitals also contribute dispersive bands around  $E_F$ . The  $d_{z^2}$  ( $A_g$ , cyan) and  $d_{xy}$  ( $B_{1g}$ , magenta) bands are very dispersive and contribute negligible DOS at  $E_F$ . There are also very dispersive Sb  $p$ -bands crossing  $E_F$  (not shown as fat-bands). It should be emphasized that the total DOS at  $E_F$  is, however, not large because those flat-band portions are away from  $E_F$ .

As shown in Table. I, our DFT+DMFT calculations yield about 4.3  $d$ -electrons per Cr-site, which are almost equally distributed among the five  $d$ -orbitals. This is nominally one-electron less than the half-filling, characteristic of Hund's metal. The quasi-particle mass-enhancement  $m^*/m^{\text{DFT}} = 1/Z$  ( $Z$  is quasi-particle weight) and effective scattering rate  $-\text{Im}\Sigma(\omega = 0)$  calcu-

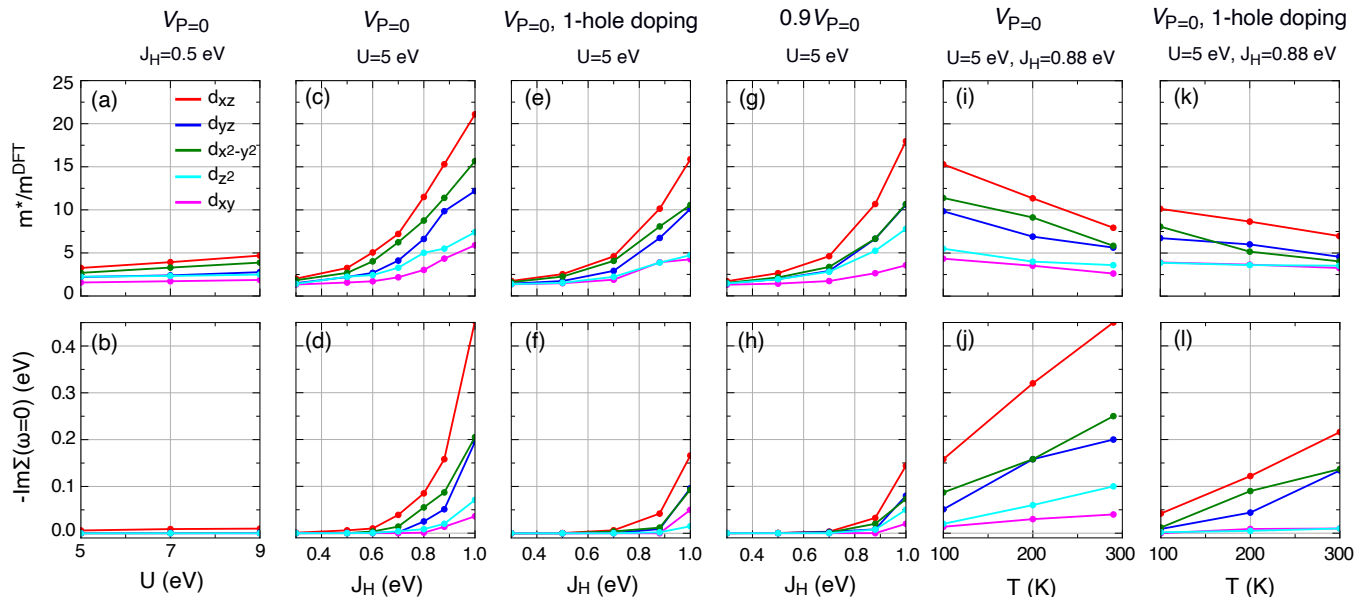


FIG. 2. Heavy-fermions in  $\text{CsCr}_3\text{Sb}_5$  revealed by DFT+DMFT calculations. Quasi-particle mass-enhancement  $m^*/m^{\text{DFT}}$  and effective scattering rate  $-\text{Im}\Sigma(\omega=0)$  as functions of (a),(b) Hubbard  $U$  at  $J_H = 0.5$  eV,  $T = 100$  K, (c)-(h) Hund's coupling  $J_H$  at  $U = 5$  eV,  $T = 100$  K, (i)-(l) and temperatures at  $U = 5$  eV,  $J_H = 0.88$  eV.

TABLE I. Occupancy of Cr  $d$ -orbitals of  $\text{CsCr}_3\text{Sb}_5$  from DFT and DFT+DMFT calculations, without and with one-hole doping. The DFT+DMFT calculations are performed at  $U=5.0$ ,  $J_H = 0.88$  eV and  $T = 100$  K.

	$d_{xz}$	$d_{yz}$	$d_{x^2-y^2}$	$d_{z^2}$	$d_{xy}$	total
DFT, no-doping	0.967	0.826	0.767	0.899	1.037	4.496
DFT, one-hole	0.904	0.840	0.728	0.917	1.060	4.449
DMFT, no-doping	0.908	0.837	0.845	0.831	0.868	4.289
DMFT, one-hole	0.890	0.827	0.811	0.828	0.872	4.228

lated by DFT+DMFT are shown in Fig. 2. At moderate  $J_H$  (0.5 eV), the largest mass-enhancement is only 2.5 ~ 5 at relatively large Hubbard  $U$  (5 ~ 9 eV) comparing to the narrow bandwidths of those incipient flat-bands ( $< 0.5$  eV) [Fig. 2(a)]. The scattering rates are almost zero [Fig. 2(b)]. These are not consistent with the bad-metal and heavy-fermion behaviors of  $\text{CsCr}_3\text{Sb}_5$  [68]. Therefore, the Hubbard  $U$  cannot induce very strong correlations even with the presence of those incipient flat-bands, in contrast to what we usually expect. As shown in Fig. 2(c), the correlations are very sensitive to Hund's coupling  $J_H$  and show very strong orbital differentiation at large  $J_H$ . The three orbitals  $d_{xz}$ ,  $d_{yz}$  and  $d_{x^2-y^2}$  that contribute the incipient flat-bands are much more correlated than the  $d_{z^2}$  and  $d_{xy}$  orbitals. At  $U=5$  eV and  $T=100$  K, very large mass-enhancement (11 ~ 21) is induced for the  $d_{xz}$  orbital at typical  $J_H$  (0.8 ~ 1.0 eV) for 3d-electron materials [29]. This indicates moderately heavy-fermions in  $\text{CsCr}_3\text{Sb}_5$ , consistent with the large  $\gamma$  observed by experiment [68]. Meanwhile, very large

scattering rate is also induced [Fig. 2(d)], which explains the bad-metal behavior [68]. On the contrary, the mass-enhancement of  $d_{z^2}$  and  $d_{xy}$  orbitals are only 3~8 at  $J_H = 0.8\sim 1.0$  eV. These results establish  $\text{CsCr}_3\text{Sb}_5$  as a typical Hund's metal, and indicate the important roles of those incipient flat-band portions in enhancing the orbital differentiation via Hund's coupling  $J_H$ .

To further reveal their roles, we apply one-hole doping and high pressure to modify their positions and bandwidths, which are shown in Figs. 1(c)-(f). The flat-bands become a little further away from  $E_F$  by one-hole doping [Figs. 1(c), (d)], and they become slightly broader and also further away from  $E_F$  under pressure [Figs. 1(e), (f)]. As a result, the correlations are significantly reduced [Figs. 2(e)-(h)]. For example, the mass-enhancement and scattering rate of  $d_{xz}$  orbital decrease by about 33% (from 15 to 10) and 73% (from 0.15 to 0.04 eV), respectively, at  $U=5$ ,  $J_H=0.88$  eV and  $T = 100$  K, by one-hole doping. The orbital differentiation also becomes weaker. We note that, as shown in Table I, the total occupancy of Cr  $d$ -orbitals decreases only by 0.05~0.06 electrons per Cr-site under one-hole doping, indicating most of the doped holes (~80%) enter Sb  $p$ -orbitals. Such small change in  $d$ -orbital occupancy can not account for such dramatic change of the correlations. Therefore, the large reduction of the correlations can only be attributed to the changes of the positions and bandwidths of those incipient flat-band portions. This indicates that the electron correlations and thus the magnetism are very sensitive to those incipient flat-band portions, so they should be one of the key factors responsible for the pressure-induced

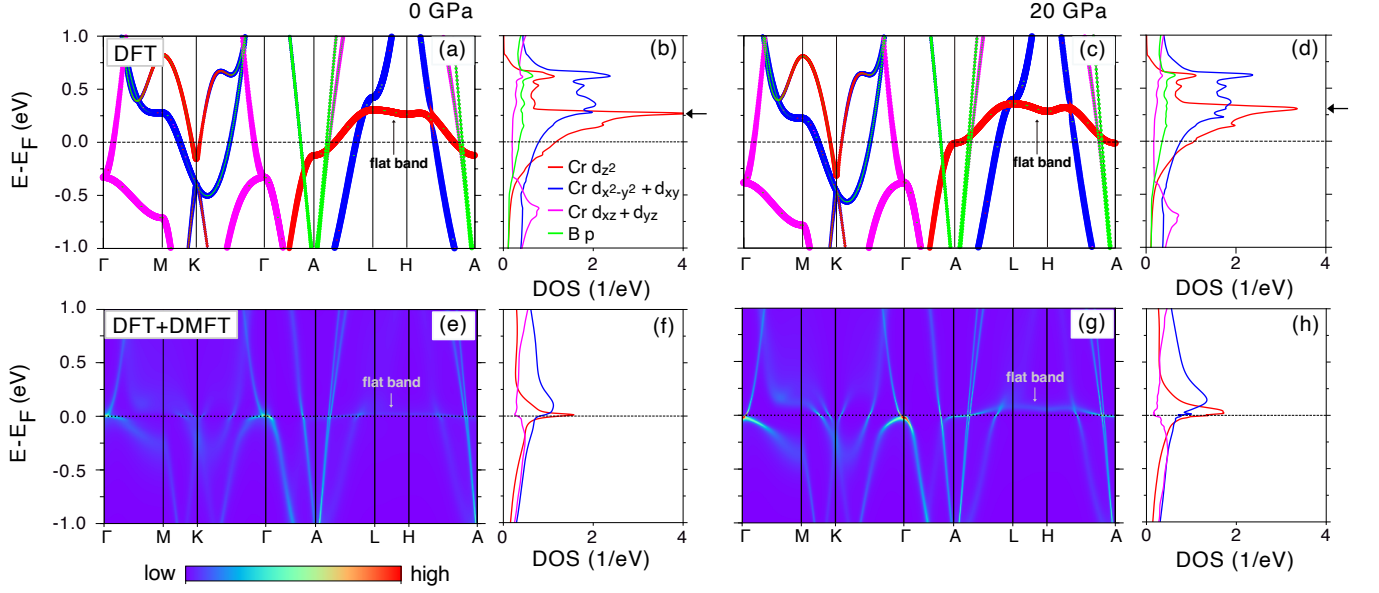


FIG. 3. Incipient flat-band in  $\text{CrB}_2$ . (a)-(d) DFT calculated band structures and DOS. (e)-(h) DFT+DMFT calculated spectra functions at  $U = 5$  eV,  $J_H = 0.9$  eV and  $T = 100$  K. (a),(b),(e),(f) Results of 0 GPa. (c),(d),(g),(h) Results of 20 GPa.

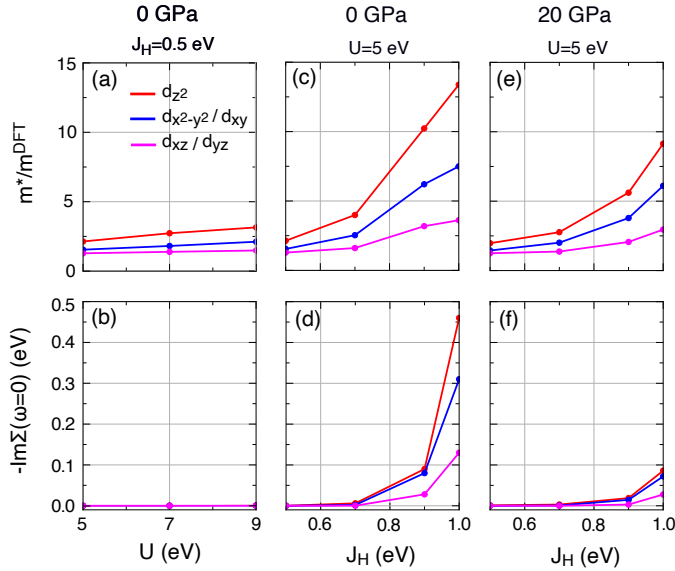


FIG. 4. Heavy-fermions in  $\text{CrB}_2$  revealed by DFT+DMFT calculations. Mass-enhancement and scattering rate as functions of (a),(b) Hubbard  $U$  at  $J_H = 0.5$  eV,  $T = 100$  K, (c)-(f) Hund's coupling  $J_H$  at  $U = 5$  eV,  $T = 100$  K.

superconductivity in  $\text{CsCr}_3\text{Sb}_5$ .

Next, we examine how the roles of the incipient flat-bands in inducing electron correlations be amplified in a Hund's metal. Model calculations have shown that  $J_H$  itself can induce large band-renormalization regardless of the band structure details in Hund's metals [26, 28]. Although the incipient flat-band portions

are initially far away from  $E_F$  in the non-interacting limit, they are pushed closer to  $E_F$  due to the  $J_H$ -induced band-renormalization [see Figs. 1(g)-(l)]. As positive feedback, they further enhance the orbital differentiation. Moreover, it is well-known that the existence of flat-bands around  $E_F$  will induce Kondo-like effect, which further enhances the inherent Kondo-like effect of Hund's metal. This is supported by the Kondo-like crossover shown in Figs. 2(i) and (j). With decreasing temperatures, the scattering rates significantly decrease [Fig. 2(j)] and quasi-particles emerge with dramatic enhancement of their mass [Fig. 2(i)]. While, the Kondo-like effect becomes weaker when the flat-bands are pushed further away from  $E_F$  by the one-hole doping [Figs. 2(k),(l)]. Consequently, the enhanced orbital differentiation and Kondo-like effect lead to the emergence of heavy-fermions.

*Heavy fermion in  $\text{CrB}_2$ .* The DFT calculated band structures and DOS of  $\text{CrB}_2$  are shown in Figs. 3(a)-(d). The Cr  $d$ -bands are split into three groups in terms of the point-group of Cr site ( $D_{6h}$ ):  $d_{z^2}$  ( $A_{1g}$ , red),  $d_{x^2-y^2}/d_{xy}$  ( $E_{2g}$ , blue) and  $d_{xz}/d_{yz}$  ( $E_{1g}$ , magenta). There are also very dispersive B  $p$ -bands (green) crossing  $E_F$ . At the BZ boundary ( $k_z = \pi$ ), there is an incipient flat-band with  $d_{z^2}$  character, which is about 0.25 eV above  $E_F$  [Figs. 3(a), (b)].

Similar to  $\text{CsCr}_3\text{Sb}_5$ , our DFT+DMFT calculations yield about 4.2  $d$ -electrons per Cr-site for  $\text{CrB}_2$ , which are distributed among the five  $d$ -orbitals (see Table S1 [78]). The mass-enhancement and scattering rate calculated by DFT+DMFT are shown in Fig. 4. At moderate  $J_H$  (0.5 eV), the largest mass-enhancement ( $d_{z^2}$  orbital) is only



2.1  $\sim$  3.1 at  $U=5 \sim 9$  eV [Fig. 4(a)], and the scattering rate is almost zero [Fig. 4(b)]. While, the electron correlations are very sensitive to  $J_H$  and show strong orbital differentiation [Figs. 4(c), (d)]. The  $d_{z^2}$  orbital that contributes the incipient flat-band is the most correlated one. For example, it has very large mass-enhancement ( $\sim 10$ ) and scattering rate at  $U=5$  eV,  $J_H=0.9$  eV,  $T=100$  K, which are consistent with the bad-metal and heavy-fermion behaviors observed by the experiment [69]. The incipient flat-band also gets much closer to  $E_F$  due to the large band renormalization [Figs. 3(e)-(h)]. Therefore,  $\text{CrB}_2$  is also a typical Hund's metal. Comparing to  $\text{CsCr}_3\text{Sb}_5$ , its correlations are relatively weaker, consistent with the values of the specific-heat coefficient  $\gamma$  [68, 69]. At 20 GPa, the most pronounced change is that the incipient flat-band becomes slightly broader and further away from  $E_F$  [Figs. 3(c), (d)], and as a result, the correlations are significantly reduced. For example, the mass-enhancement of  $d_{z^2}$  orbital decreases by 45% (from 10.2 to 5.6) [Figs. 4(e)]. The orbital differentiation also becomes weaker. This again indicates the important roles of the incipient flat-bands in driving the strong electron correlations and heavy-fermions.

*Conclusion and Discussion.* To summarize, our calculations show that the combination of Hund's correlations and portions of incipient flat-bands can lead to very strong electron correlations and even heavy-fermions, by enhancing the orbital differentiation and inherent Kondo-like effect of Hund's metals. The kagome  $\text{CsCr}_3\text{Sb}_5$  and triangular  $\text{CrB}_2$  are such cases, which explains the origin of their bad-metal and heavy-fermions behaviors observed by experiments [68, 69]. It thus provides a flexible route for generating  $d$ -electron heavy-fermions in frustrated Hund's metal.

Previous studies suggest that incipient flat-bands are helpful for enhancing electron pairing [25, 79–81], so they may be crucial for the pressure-induced superconductivity in  $\text{CsCr}_3\text{Sb}_5$  and  $\text{CrB}_2$ . Moreover, the AFM fluctuations are strong in the frustrated lattices. Therefore, frustrated Hund's metals with incipient flat-bands provide a good environment suitable for the emergence of unconventional superconductivity. A large family of materials with kagome, triangular, pyrochlore lattices consisting of Cr ( $d^4$ ), Ru ( $d^4$ ), Fe ( $d^6$ ) ions are promising candidates.

In reality, the one-hole doping in  $\text{CsCr}_3\text{Sb}_5$  can be realized by replacing one Sb-site with Ge, which is shown in the Fig. S1 and Table. S2 [78]. This leads to very similar changes of the positions of incipient flat-bands, the total occupancy of Cr  $d$ -orbitals and the electron correlations, to those by the uniform one-hole doping. Since the correlations have been reduced, the AFM order may be destroyed and the superconductivity may be realized in  $\text{CsCr}_3\text{Sb}_4\text{Ge}$  at ambient pressure.

*Note added.* Recently, we learned that another paradigm for finding  $d$ -electron heavy-fermions based on

Hund's metal has been proposed by Crispino *et. al.* [82], by doping towards half-filling of a Hund's metal to enhance the orbital differentiation and reach extremely heavy mass-enhancements with a given orbital character.

*Acknowledgement.* This project was supported by the Innovation Program for Quantum Science and Technology (No. 2021ZD0302800), the National Natural Science Foundation of China (No. 12174365) and the New Cornerstone Science Foundation. All the calculations were performed on TianHe-1(A), the National Supercomputer Center in Tianjin, China.

\* yilinwang@ustc.edu.cn

- [1] Masatoshi Imada, Atsushi Fujimori, and Yoshinori Tokura, "Metal-insulator transitions," *Rev. Mod. Phys.* **70**, 1039–1263 (1998).
- [2] D. C. Tsui, H. L. Stormer, and A. C. Gossard, "Two-dimensional magnetotransport in the extreme quantum limit," *Phys. Rev. Lett.* **48**, 1559–1562 (1982).
- [3] R. B. Laughlin, "Anomalous quantum hall effect: An incompressible quantum fluid with fractionally charged excitations," *Phys. Rev. Lett.* **50**, 1395–1398 (1983).
- [4] Evelyn Tang, Jia-Wei Mei, and Xiao-Gang Wen, "High-temperature fractional quantum hall states," *Phys. Rev. Lett.* **106**, 236802 (2011).
- [5] N. Regnault and B. Andrei Bernevig, "Fractional chern insulator," *Phys. Rev. X* **1**, 021014 (2011).
- [6] Rafi Bistritzer and Allan H. MacDonald, "Moiré bands in twisted double-layer graphene," *Proceedings of the National Academy of Sciences* **108**, 12233–12237 (2011).
- [7] Yuan Cao, Valla Fatemi, Ahmet Demir, Shiang Fang, Spencer L. Tomarken, Jason Y. Luo, Javier D. Sanchez-Yamagishi, Kenji Watanabe, Takashi Taniguchi, Efthimios Kaxiras, Ray C. Ashoori, and Pablo Jarillo-Herrero, "Correlated insulator behaviour at half-filling in magic-angle graphene superlattices," *Nature* **556**, 80–84 (2018).
- [8] G. R. Stewart, "Heavy-fermion systems," *Rev. Mod. Phys.* **56**, 755–787 (1984).
- [9] Piers Coleman, "Heavy fermions: Electrons at the edge of magnetism," (John Wiley & Sons, Ltd, 2007).
- [10] Qimiao Si and Frank Steglich, "Heavy fermions and quantum phase transitions," *Science* **329**, 1161–1166 (2010).
- [11] Itiro Syôzi, "Statistics of Kagomé Lattice," *Progress of Theoretical Physics* **6**, 306–308 (1951).
- [12] A Mielke, "Ferromagnetic ground states for the hubbard model on line graphs," *Journal of Physics A: Mathematical and General* **24**, L73 (1991).
- [13] Subir Sachdev, "Kagome- and triangular-lattice Heisenberg antiferromagnets: Ordering from quantum fluctuations and quantum-disordered ground states with unconfined bosonic spinons," *Phys. Rev. B* **45**, 12377–12396 (1992).
- [14] Nicolas Regnault, Yuanfeng Xu, Ming-Rui Li, Da-Shuai Ma, Milena Jovanovic, Ali Yazdani, Stuart S. P. Parkin, Claudia Felser, Leslie M. Schoop, N. Phuan Ong, Robert J. Cava, Luis Elcoro, Zhi-Da Song, and B. Andrei

- Bernevig, “Catalogue of flat-band stoichiometric materials,” *Nature* **603**, 824–828 (2022).
- [15] Zhonghao Liu, Man Li, Qi Wang, Guangwei Wang, Chenhaoping Wen, Kun Jiang, Xiangle Lu, Shichao Yan, Yaobo Huang, Dawei Shen, Jia-Xin Yin, Ziqiang Wang, Zhiping Yin, Hechang Lei, and Shancai Wang, “Orbital-selective dirac fermions and extremely flat bands in frustrated kagome-lattice metal CoSn,” *Nature Communications* **11**, 4002 (2020).
- [16] Mingu Kang, Linda Ye, Shiang Fang, Jhih-Shih You, Abe Levitan, Minyong Han, Jorge I. Facio, Chris Jozwiak, Aaron Bostwick, Eli Rotenberg, Mun K. Chan, Ross D. McDonald, David Graf, Konstantine Kaznatcheev, Elio Vescovo, David C. Bell, Efthimios Kaxiras, Jeroen van den Brink, Manuel Richter, Madhav Prasad Ghimire, Joseph G. Checkelsky, and Riccardo Comin, “Dirac fermions and flat bands in the ideal kagome metal FeSn,” *Nature Materials* **19**, 163–169 (2020).
- [17] Hao Huang, Lixuan Zheng, Zhiyong Lin, Xu Guo, Sheng Wang, Shuai Zhang, Chi Zhang, Zhe Sun, Zhengfei Wang, Hongming Weng, Lin Li, Tao Wu, Xianhui Chen, and Changgan Zeng, “Flat-band-induced anomalous anisotropic charge transport and orbital magnetism in kagome metal CoSn,” *Phys. Rev. Lett.* **128**, 096601 (2022).
- [18] Zhiyong Lin, Jin-Ho Choi, Qiang Zhang, Wei Qin, Seho Yi, Pengdong Wang, Lin Li, Yifan Wang, Hui Zhang, Zhe Sun, Laiming Wei, Shengbai Zhang, Tengfei Guo, Qingyou Lu, Jun-Hyung Cho, Changgan Zeng, and Zhenyu Zhang, “Flatbands and emergent ferromagnetic ordering in  $\text{Fe}_3\text{Sn}_2$  kagome lattices,” *Phys. Rev. Lett.* **121**, 096401 (2018).
- [19] Mingu Kang, Shiang Fang, Linda Ye, Hoi Chun Po, Jonathan Denlinger, Chris Jozwiak, Aaron Bostwick, Eli Rotenberg, Efthimios Kaxiras, Joseph G. Checkelsky, and Riccardo Comin, “Topological flat bands in frustrated kagome lattice CoSn,” *Nature Communications* **11**, 4004 (2020).
- [20] Jia-Xin Yin, Songtian S. Zhang, Guoqing Chang, Qi Wang, Stepan S. Tsirkin, Zurab Guguchia, Biao Lian, Huibin Zhou, Kun Jiang, Ilya Belopolski, Nana Shumiya, Daniel Multer, Maksim Litskevich, Tyler A. Cochran, Hsin Lin, Ziqiang Wang, Titus Neupert, Shuang Jia, Hechang Lei, and M. Zahid Hasan, “Negative flat band magnetism in a spin-orbit-coupled correlated kagome magnet,” *Nature Physics* **15**, 443–448 (2019).
- [21] Jia-Xin Yin, Biao Lian, and M. Zahid Hasan, “Topological kagome magnets and superconductors,” *Nature* **612**, 647–657 (2022).
- [22] Li Huang and Haiyan Lu, “Signatures of hundness in kagome metals,” *Phys. Rev. B* **102**, 125130 (2020).
- [23] Maximilian L. Kiesel, Christian Platt, and Ronny Thomale, “Unconventional fermi surface instabilities in the kagome hubbard model,” *Phys. Rev. Lett.* **110**, 126405 (2013).
- [24] William R. Meier, Mao-Hua Du, Satoshi Okamoto, Narayan Mohanta, Andrew F. May, Michael A. McGuire, Craig A. Bridges, German D. Samolyuk, and Brian C. Sales, “Flat bands in the CoSn-type compounds,” *Phys. Rev. B* **102**, 075148 (2020).
- [25] Hideo Aoki, “Theoretical possibilities for flat band superconductivity,” *Journal of Superconductivity and Novel Magnetism* **33**, 2341–2346 (2020).
- [26] Philipp Werner, Emanuel Gull, Matthias Troyer, and Andrew J. Millis, “Spin freezing transition and non-fermi-liquid self-energy in a three-orbital model,” *Phys. Rev. Lett.* **101**, 166405 (2008).
- [27] K Haule and G Kotliar, “Coherence-incoherence crossover in the normal state of iron oxyphnictides and importance of Hund’s rule coupling,” *New Journal of Physics* **11**, 025021 (2009).
- [28] Luca de’ Medici, Jernej Mravlje, and Antoine Georges, “Janus-faced influence of Hund’s rule coupling in strongly correlated materials,” *Phys. Rev. Lett.* **107**, 256401 (2011).
- [29] Z. P. Yin, K. Haule, and G. Kotliar, “Kinetic frustration and the nature of the magnetic and paramagnetic states in iron pnictides and iron chalcogenides,” *Nature Materials* **10**, 932 (2011).
- [30] Z. P. Yin, K. Haule, and G. Kotliar, “Magnetism and charge dynamics in iron pnictides,” *Nature Physics* **7**, 294–297 (2011).
- [31] Z. P. Yin, K. Haule, and G. Kotliar, “Fractional power-law behavior and its origin in iron-chalcogenide and ruthenate superconductors: Insights from first-principles calculations,” *Phys. Rev. B* **86**, 195141 (2012).
- [32] Antoine Georges, Luca de’ Medici, and Jernej Mravlje, “Strong correlations from Hund’s coupling,” *Annual Review of Condensed Matter Physics* **4**, 137–178 (2013).
- [33] K. M. Stadler, Z. P. Yin, J. von Delft, G. Kotliar, and A. Weichselbaum, “Dynamical mean-field theory plus numerical renormalization-group study of spin-orbital separation in a three-band hund metal,” *Phys. Rev. Lett.* **115**, 136401 (2015).
- [34] K.M. Stadler, G. Kotliar, A. Weichselbaum, and J. von Delft, “Hundness versus Mottness in a three-band Hubbard–Hund model: On the origin of strong correlations in Hund metals,” *Annals of Physics* **405**, 365 – 409 (2019).
- [35] Siheon Ryee, Myung Joon Han, and Sangkook Choi, “Hund physics landscape of two-orbital systems,” *Phys. Rev. Lett.* **126**, 206401 (2021).
- [36] Y. Wang, C.-J. Kang, H. Miao, and G. Kotliar, “Hund’s metal physics: From  $\text{SrNiO}_2$  to  $\text{LaNiO}_2$ ,” *Phys. Rev. B* **102**, 161118 (2020).
- [37] Chang-Jong Kang and Gabriel Kotliar, “Optical properties of the infinite-layer  $\text{La}_{1-x}\text{Sr}_x\text{NiO}_2$  and hidden hund’s physics,” *Phys. Rev. Lett.* **126**, 127401 (2021).
- [38] Taek Jung Kim, Siheon Ryee, and Myung Joon Han, “ $\text{Fe}_3\text{GeTe}_2$ : a site-differentiated hund metal,” *npj Computational Materials* **8**, 245 (2022).
- [39] A. A. Schafgans, S. J. Moon, B. C. Pursley, A. D. LaForge, M. M. Qazilbash, A. S. Sefat, D. Mandrus, K. Haule, G. Kotliar, and D. N. Basov, “Electronic correlations and unconventional spectral weight transfer in the high-temperature pnictide  $\text{BaFe}_{2-x}\text{Co}_x\text{As}_2$  superconductor using infrared spectroscopy,” *Phys. Rev. Lett.* **108**, 147002 (2012).
- [40] Luca de’ Medici, “Hund’s induced fermi-liquid instabilities and enhanced quasiparticle interactions,” *Phys. Rev. Lett.* **118**, 167003 (2017).
- [41] Cyrus F. Hirjibehedin, “The makings of a hund’s metal,” *Nature Nanotechnology* **10**, 914–915 (2015).
- [42] Luca de’ Medici, “Hund’s metals, explained,” (2017), [arXiv:1707.03282](https://arxiv.org/abs/1707.03282).
- [43] F. Hardy, A. E. Böhmer, D. Aoki, P. Burger, T. Wolf, P. Schweiss, R. Heid, P. Adelmann, Y. X. Yao, G. Kotliar, J. Schmalian, and C. Meingast, “Evidence of strong correlations and coherence-incoherence crossover in the

- iron pnictide superconductor  $\text{KFe}_2\text{As}_2$ ,” *Phys. Rev. Lett.* **111**, 027002 (2013).
- [44] M. Yi, D. H. Lu, R. Yu, S. C. Riggs, J.-H. Chu, B. Lv, Z. K. Liu, M. Lu, Y.-T. Cui, M. Hashimoto, S.-K. Mo, Z. Hussain, C. W. Chu, I. R. Fisher, Q. Si, and Z.-X. Shen, “Observation of temperature-induced crossover to an orbital-selective mott phase in  $\text{A}_x\text{Fe}_{2-y}\text{Se}_2$  ( $\text{A}=\text{K}, \text{Rb}$ ) superconductors,” *Phys. Rev. Lett.* **110**, 067003 (2013).
- [45] Nicola Lanatà, Hugo U. R. Strand, Gianluca Giovannetti, Bo Hellsing, Luca de’ Medici, and Massimo Capone, “Orbital selectivity in hund’s metals: The iron chalcogenides,” *Phys. Rev. B* **87**, 045122 (2013).
- [46] Jernej Mravlje, Markus Aichhorn, Takashi Miyake, Kristjan Haule, Gabriel Kotliar, and Antoine Georges, “Coherence-incoherence crossover and the mass-renormalization puzzles in  $\text{Sr}_2\text{RuO}_4$ ,” *Phys. Rev. Lett.* **106**, 096401 (2011).
- [47] Xiaoyu Deng, Kristjan Haule, and Gabriel Kotliar, “Transport properties of metallic ruthenates: A DFT + DMFT investigation,” *Phys. Rev. Lett.* **116**, 256401 (2016).
- [48] Takeshi Kondo, M. Ochi, M. Nakayama, H. Taniguchi, S. Akebi, K. Kuroda, M. Arita, S. Sakai, H. Namatame, M. Taniguchi, Y. Maeno, R. Arita, and S. Shin, “Orbital-dependent band narrowing revealed in an extremely correlated hund’s metal emerging on the topmost layer of  $\text{Sr}_2\text{RuO}_4$ ,” *Phys. Rev. Lett.* **117**, 247001 (2016).
- [49] Jonathan Karp, Max Bramberger, Martin Grundner, Ulrich Schollwöck, Andrew J. Millis, and Manuel Zingl, “ $\text{Sr}_2\text{MoO}_4$  and  $\text{Sr}_2\text{RuO}_4$ : Disentangling the roles of hund’s and van hove physics,” *Phys. Rev. Lett.* **125**, 166401 (2020).
- [50] Minjae Kim, Jernej Mravlje, Michel Ferrero, Olivier Parcollet, and Antoine Georges, “Spin-orbit coupling and electronic correlations in  $\text{Sr}_2\text{RuO}_4$ ,” *Phys. Rev. Lett.* **120**, 126401 (2018).
- [51] Luca de’ Medici, S. R. Hassan, Massimo Capone, and Xi Dai, “Orbital-selective mott transition out of band degeneracy lifting,” *Phys. Rev. Lett.* **102**, 126401 (2009).
- [52] Fabian B. Kugler, Seung-Sup B. Lee, Andreas Weichselbaum, Gabriel Kotliar, and Jan von Delft, “Orbital differentiation in hund metals,” *Phys. Rev. B* **100**, 115159 (2019).
- [53] Philipp Werner and Andrew J. Millis, “High-spin to low-spin and orbital polarization transitions in multiorbital mott systems,” *Phys. Rev. Lett.* **99**, 126405 (2007).
- [54] M. Yi, Z.-K. Liu, Y. Zhang, R. Yu, J.-X. Zhu, J. J. Lee, R. G. Moore, F. T. Schmitt, W. Li, S. C. Riggs, J.-H. Chu, B. Lv, J. Hu, M. Hashimoto, S.-K. Mo, Z. Hussain, Z. Q. Mao, C. W. Chu, I. R. Fisher, Q. Si, Z.-X. Shen, and D. H. Lu, “Observation of universal strong orbital-dependent correlation effects in iron chalcogenides,” *Nature Communications* **6**, 7777 (2015).
- [55] A. Kostin, P. O. Sprau, A. Kreisler, Yi Xue Chong, A. E. Böhmer, P. C. Canfield, P. J. Hirschfeld, B. M. Andersen, and J. C. Séamus Davis, “Imaging orbital-selective quasiparticles in the hund’s metal state of  $\text{FeSe}$ ,” *Nature Materials* **17**, 869–874 (2018).
- [56] Nicola Lanatà, Hugo U. R. Strand, Gianluca Giovannetti, Bo Hellsing, Luca de’ Medici, and Massimo Capone, “Orbital selectivity in hund’s metals: The iron chalcogenides,” *Phys. Rev. B* **87**, 045122 (2013).
- [57] Manuel Zingl, Jernej Mravlje, Markus Aichhorn, Olivier Parcollet, and Antoine Georges, “Hall coefficient signals orbital differentiation in the hund’s metal  $\text{Sr}_2\text{RuO}_4$ ,” *npj Quantum Materials* **4**, 35 (2019).
- [58] Akihisa Koga, Norio Kawakami, T. M. Rice, and Manfred Sigrist, “Spin, charge, and orbital fluctuations in a multiorbital mott insulator,” *Phys. Rev. B* **72**, 045128 (2005).
- [59] Akihisa Koga, Norio Kawakami, T. M. Rice, and Manfred Sigrist, “Orbital-selective mott transitions in the degenerate hubbard model,” *Phys. Rev. Lett.* **92**, 216402 (2004).
- [60] Fabian B. Kugler and Gabriel Kotliar, “Is the orbital-selective mott phase stable against interorbital hopping?” *Phys. Rev. Lett.* **129**, 096403 (2022).
- [61] Y. Wang, E. Walter, S.-S. B. Lee, K. M. Stadler, J. von Delft, A. Weichselbaum, and G. Kotliar, “Global phase diagram of a spin-orbital kondo impurity model and the suppression of fermi-liquid scale,” *Phys. Rev. Lett.* **124**, 136406 (2020).
- [62] Andriy H. Nevidomskyy and P. Coleman, “Kondo resonance narrowing in  $d$ - and  $f$ -electron systems,” *Phys. Rev. Lett.* **103**, 147205 (2009).
- [63] Antoine Georges, Gabriel Kotliar, Werner Krauth, and Marcelo J. Rozenberg, “Dynamical mean-field theory of strongly correlated fermion systems and the limit of infinite dimensions,” *Rev. Mod. Phys.* **68**, 13–125 (1996).
- [64] G. Kotliar, S. Y. Savrasov, K. Haule, V. S. Oudovenko, O. Parcollet, and C. A. Marianetti, “Electronic structure calculations with dynamical mean-field theory,” *Rev. Mod. Phys.* **78**, 865–951 (2006).
- [65] A. I. Lichtenstein, M. I. Katsnelson, and G. Kotliar, “Finite-temperature magnetism of transition metals: An ab initio dynamical mean-field theory,” *Phys. Rev. Lett.* **87**, 067205 (2001).
- [66] Brenden R. Ortiz, Lídia C. Gomes, Jennifer R. Morey, Michal Winiarski, Mitchell Bordelon, John S. Mangum, Iain W. H. Oswald, Jose A. Rodriguez-Rivera, James R. Neilson, Stephen D. Wilson, Elif Ertekin, Tyrel M. McQueen, and Eric S. Toberer, “New kagome prototype materials: discovery of  $\text{KV}_3\text{Sb}_5$ ,  $\text{RbV}_3\text{Sb}_5$  and  $\text{CsV}_3\text{Sb}_5$ ,” *Phys. Rev. Mater.* **3**, 094407 (2019).
- [67] Brenden R. Ortiz, Samuel M. L. Teicher, Yong Hu, Julia L. Zuo, Paul M. Sarte, Emily C. Schueller, A. M. Milinda Abeykoon, Matthew J. Krogstad, Stephan Rosenkranz, Raymond Osborn, Ram Seshadri, Leon Balents, Junfeng He, and Stephen D. Wilson, “ $\text{CsV}_3\text{Sb}_5$ : A  $\text{Z}_2$  topological kagome metal with a superconducting ground state,” *Phys. Rev. Lett.* **125**, 247002 (2020).
- [68] Yi Liu, Zi-Yi Liu, Jin-Ke Bao, Peng-Tao Yang, Liang-Wen Ji, Ji-Yong Liu, Chen-Chao Xu, Wu-Zhang Yang, Wan-Li Chai, Jia-Yi Lu, Chang-Chao Liu, Bo-Sen Wang, Hao Jiang, Qian Tao, Zhi Ren, Xiao-Feng Xu, Chao Cao, Zhu-An Xu, Jin-Guang Cheng, and Guang-Han Cao, “Superconductivity emerged from density-wave order in a kagome bad metal,” (2023), [arXiv:2309.13514](https://arxiv.org/abs/2309.13514).
- [69] A. Bauer, A. Regnat, C. G. F. Blum, S. Gottlieb-Schönmeier, B. Pedersen, M. Meven, S. Wurmehl, J. Kuneš, and C. Pfeleiderer, “Low-temperature properties of single-crystal  $\text{CrB}_2$ ,” *Phys. Rev. B* **90**, 064414 (2014).
- [70] Chenchao Xu, Siqi Wu, Guo-Xiang Zhi, Guanghan Cao, Jianhui Dai, Chao Cao, Xiaoqun Wang, and Hai-Qing Lin, “Frustrated altermagnetism and charge density wave in kagome superconductor  $\text{CsCr}_3\text{Sb}_5$ ,” (2023),

- [arXiv:2309.14812](#).
- [71] Cuiying Pei, Pengtao Yang, Chunsheng Gong, Qi Wang, Yi Zhao, Lingling Gao, Keyu Chen, Qiangwei Yin, Shangjie Tian, Changhua Li, Weizheng Cao, Hechang Lei, Jinguang Cheng, and Yanpeng Qi, “Pressure-induced superconductivity in itinerant antiferromagnet  $\text{CrB}_2$ ,” (2021), [arXiv:2109.15213](#).
- [72] Sananda Biswas, Andreas Kreisel, Adrian Valadkhani, Matteo Dürrnagel, Tilman Schwemmer, Ronny Thomale, Roser Valenti, and Igor I. Mazin, “Hybrid  $s$ -wave superconductivity in  $\text{CrB}_2$ ,” *Phys. Rev. B* **108**, L020501 (2023).
- [73] Kristjan Haule, Chuck-Hou Yee, and Kyoo Kim, “Dynamical mean-field theory within the full-potential methods: Electronic structure of  $\text{CeIrIn}_5$ ,  $\text{CeCoIn}_5$ , and  $\text{CeRhIn}_5$ ,” *Phys. Rev. B* **81**, 195107 (2010).
- [74] Kristjan Haule and Turan Birol, “Free energy from stationary implementation of the DFT+DMFT functional,” *Phys. Rev. Lett.* **115**, 256402 (2015).
- [75] Peter Blaha, Karlheinz Schwarz, Fabien Tran, Robert Laskowski, Georg K. H. Madsen, and Laurence D. Marks, “WIEN2k: An APW+lo program for calculating the properties of solids,” *The Journal of Chemical Physics* **152**, 074101 (2020).
- [76] Kristjan Haule, “Exact double counting in combining the dynamical mean field theory and the density functional theory,” *Phys. Rev. Lett.* **115**, 196403 (2015).
- [77] Emanuel Gull, Andrew J. Millis, Alexander I. Liechtenstein, Alexey N. Rubtsov, Matthias Troyer, and Philipp Werner, “Continuous-time monte carlo methods for quantum impurity models,” *Rev. Mod. Phys.* **83**, 349–404 (2011).
- [78] See Supporting Information at [url] for: (1) Computational details, (2) Results of  $\text{CsCr}_3\text{Sb}_4\text{Ge}$ ..
- [79] Karin Matsumoto, Daisuke Ogura, and Kazuhiko Kuroki, “Wide applicability of high- $T_c$  pairing originating from coexisting wide and incipient narrow bands in quasi-one-dimensional systems,” *Phys. Rev. B* **97**, 014516 (2018).
- [80] Daisuke Ogura, Hideo Aoki, and Kazuhiko Kuroki, “Possible high- $T_c$  superconductivity due to incipient narrow bands originating from hidden ladders in ruddlesden-popper compounds,” *Phys. Rev. B* **96**, 184513 (2017).
- [81] Karin Matsumoto, Daisuke Ogura, and Kazuhiko Kuroki, “Strongly enhanced superconductivity due to finite energy spin fluctuations induced by an incipient band: A flex study on the bilayer hubbard model with vertical and diagonal interlayer hoppings,” *Journal of the Physical Society of Japan* **89**, 044709 (2020).
- [82] Matteo Crispino, Pablo Villar Arribi, Anmol Shukla, Frédéric Hardy, Amir-Abbas Haghighirad, Thomas Wolf, Rolf Heid, Christoph Meingast, Tommaso Gorni, Adolfo Avella, and Luca de’ Medici, “Paradigm for finding  $d$ -electron heavy fermions: the case of Cr-doped  $\text{CsFe}_2\text{As}_2$ ,” (2023), [arXiv:2312.06511](#).



# Supplementary Materials for “Heavy-fermion in frustrated Hund’s metal with portions of incipient flat-bands”

Yilin Wang<sup>1,2,3,\*</sup>

<sup>1</sup>*Hefei National Research Center for Interdisciplinary Sciences at the Microscale,  
University of Science and Technology of China, Hefei 230026, China*

<sup>2</sup>*Hefei National Laboratory, University of Science and Technology of China, Hefei 230088, China*

<sup>3</sup>*New Cornerstone Science Laboratory, University of Science and Technology of China, Hefei, 230026, China*

(Dated: January 31, 2024)

arXiv:2401.16770v1 [cond-mat.str-el] 30 Jan 2024

---

\* [yilinwang@ustc.edu.cn](mailto:yilinwang@ustc.edu.cn)

TABLE S1. Occupancy of Cr  $d$ -orbitals of CrB<sub>2</sub> from DFT and DFT+DMFT calculations at P=0 GPa. The DFT+DMFT calculations are performed at  $U=5.0$ ,  $J_H=0.9$  eV and  $T=100$  K.

	$d_{z^2}$	$d_{xz}$	$d_{yz}$	$d_{x^2-y^2}$	$d_{xy}$	total
DFT	0.870	0.884	0.884	0.892	0.892	4.422
DMFT	0.931	0.850	0.850	0.780	0.780	4.191

TABLE S2. Occupancy of Cr  $d$ -orbitals of CsCr<sub>3</sub>Sb<sub>5</sub> and CsCr<sub>3</sub>Sb<sub>4</sub>Ge from DFT and DFT+DMFT calculations. The DFT+DMFT calculations are performed at  $U=5.0$ ,  $J_H=0.88$  eV and  $T=100$  K.

	$d_{xz}$	$d_{yz}$	$d_{x^2-y^2}$	$d_{z^2}$	$d_{xy}$	total
CsCr <sub>3</sub> Sb <sub>5</sub> , DFT	0.967	0.826	0.767	0.899	1.037	4.496
CsCr <sub>3</sub> Sb <sub>4</sub> Ge, DFT	0.904	0.840	0.729	0.927	1.058	4.458
CsCr <sub>3</sub> Sb <sub>5</sub> , DMFT	0.908	0.837	0.845	0.831	0.868	4.289
CsCr <sub>3</sub> Sb <sub>4</sub> Ge, DMFT	0.891	0.832	0.810	0.832	0.871	4.236

### S-I. Computational Details

The crystal structures of CsCr<sub>3</sub>Sb<sub>5</sub> and CrB<sub>2</sub> are shown in Fig. S1(a) and Fig. S2(a), respectively. The experimental lattice parameters of CsCr<sub>3</sub>Sb<sub>5</sub> at ambient pressure are  $a = 5.4909$  Å,  $c = 9.2417$  Å [1]. The experimental lattice parameters of CrB<sub>2</sub> at P=0 and 20 GPa are,  $a = 2.968$  Å,  $c = 3.055$  and  $a = 2.932$  Å,  $c = 2.967$  Å, respectively [2]. For DFT+DMFT calculations,  $19 \times 19 \times 10$  and  $16 \times 16 \times 14$  K-point grid are used for CsCr<sub>3</sub>Sb<sub>5</sub> and CrB<sub>2</sub>, respectively. The RMT values for CsCr<sub>3</sub>Sb<sub>5</sub> are Cs (2.5), Cr (2.36), Sb (2.48) at ambient pressure with  $V_{P=0}$ , and Cs (2.5), Cr (2.27), Sb (2.39) at high pressure with  $0.9V_{P=0}$ . The RMT values for CrB<sub>2</sub> are Cr (2.43), B (1.61) at  $P=0$  GPa, and Cr (2.38), B (1.59) at  $P=20$  GPa. The value of Rmt\*Kmax is 7.0.

We use a local Coulomb interaction Hamiltonian with rotationally invariant form for CsCr<sub>3</sub>Sb<sub>5</sub>. It turns out that, in CrB<sub>2</sub>, the acceptance ratio of quantum Monte Carlo is very low at  $T=100$  K, such that the measurements of green's function and self-energy are very noise for rotationally invariant form of Coulomb interaction. Therefore, we use an Ising form for CrB<sub>2</sub>, which can significantly improve the acceptance ratio. Comparing to the rotationally invariant form, the Ising form will overestimate the scattering rate but underestimate the quasi-particle mass-enhancement, so it will not change the conclusion that CrB<sub>2</sub> is a moderately  $d$ -electron heavy-fermion. At  $T=100$  K, we perform a total quantum Monte Carlo sampling of  $2.56 \times 10^{10}$  to reach sufficient numerical accuracy. The mass-enhancement is calculated via real-frequency self-energy  $m^*/m^{\text{DFT}} = 1 - \frac{\partial \text{Re}\Sigma(\omega)}{\partial \omega} \Big|_{\omega \rightarrow 0}$ .

### S-II. Results of CsCr<sub>3</sub>Sb<sub>4</sub>Ge

In reality, the one-hole doping can be realized by replacing the Sb-site in the kagome layer with Ge, which is shown in Fig. S1(b). The DFT calculated band structure of CsCr<sub>3</sub>Sb<sub>4</sub>Ge is shown in Fig. S1(e), which is similar to that of uniform one-hole doping shown in the main text. Comparing to CsCr<sub>3</sub>Sb<sub>5</sub>, the incipient flat-bands are pushed a little further away from  $E_F$ . The calculated occupancy of Cr  $d$ -orbitals are shown in Table S2. Both DFT and DFT+DMFT calculations show that the total occupancy of Cr  $d$ -orbitals decreases by only 0.05~0.06 per Cr-site, which is the same as the changes induced by the uniform one-hole doping. This confirms the conclusion that most of the doped holes enter Sb/Ge  $p$ -orbitals and the large reduction of electron correlations can only be attributed to the incipient flat-bands. The DFT+DMFT calculated quasi-particle mass-enhancement of CsCr<sub>3</sub>Sb<sub>4</sub>Ge is shown in Fig. S1(h), which is almost the same as those of the uniform one-hole doping shown in the Fig.2(e) of the main text.

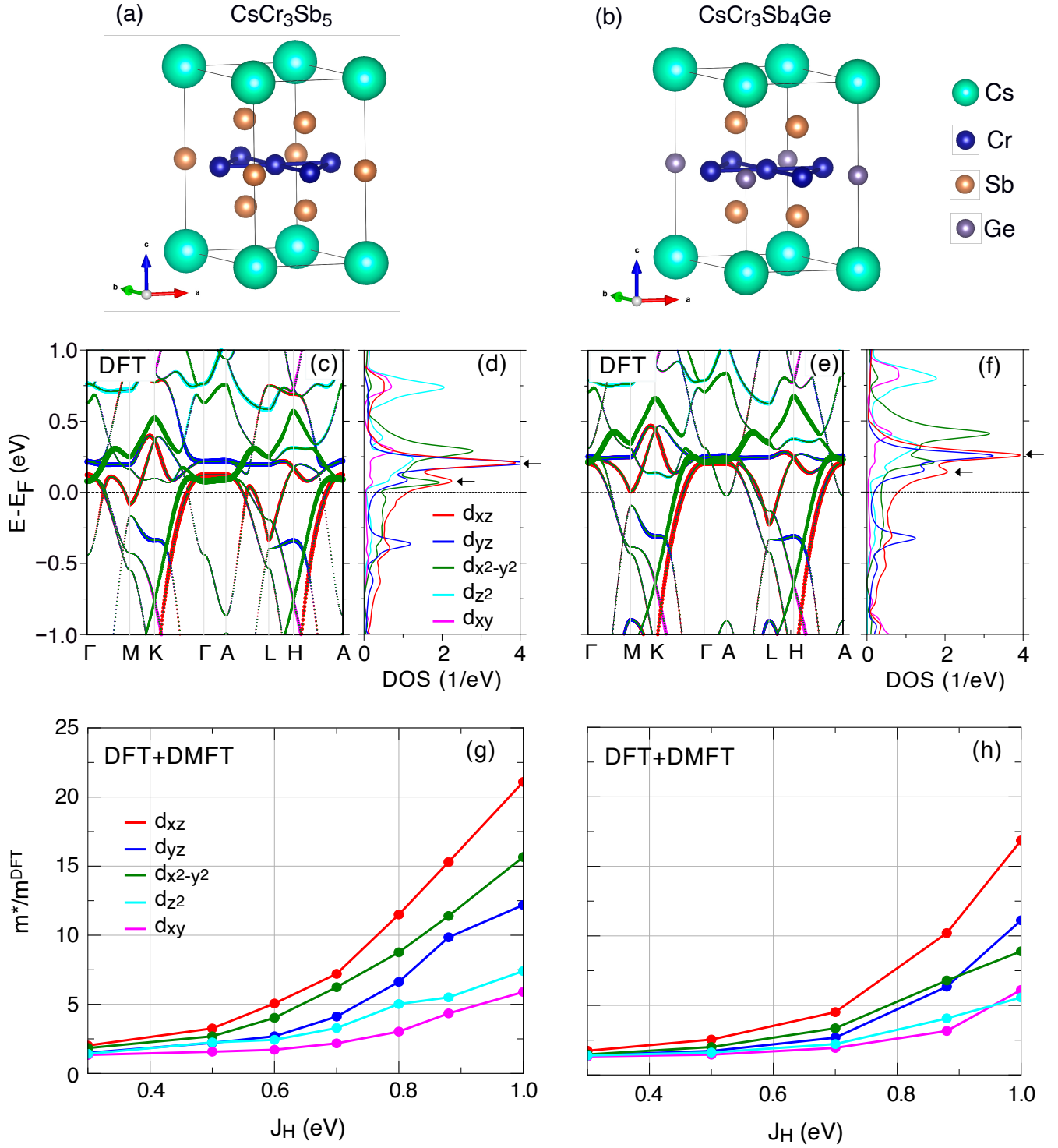


FIG. S1. Crystal structures of (a) CsCr<sub>3</sub>Sb<sub>5</sub> and (b) CsCr<sub>3</sub>Sb<sub>4</sub>Ge. The Sb-site in kagome layer is replaced with Ge in CsCr<sub>3</sub>Sb<sub>4</sub>Ge. (c)-(f) DFT calculated band structures and DOS for CsCr<sub>3</sub>Sb<sub>5</sub> and CsCr<sub>3</sub>Sb<sub>4</sub>Ge, respectively. (g),(h) The DFT+DMFT calculated quasi-particle mass-enhancement  $m^*/m^{\text{DFT}}$  for CsCr<sub>3</sub>Sb<sub>5</sub> and CsCr<sub>3</sub>Sb<sub>4</sub>Ge, resistivity, at  $U = 5$  eV,  $J_H = 0.88$  eV,  $T = 100$  K.

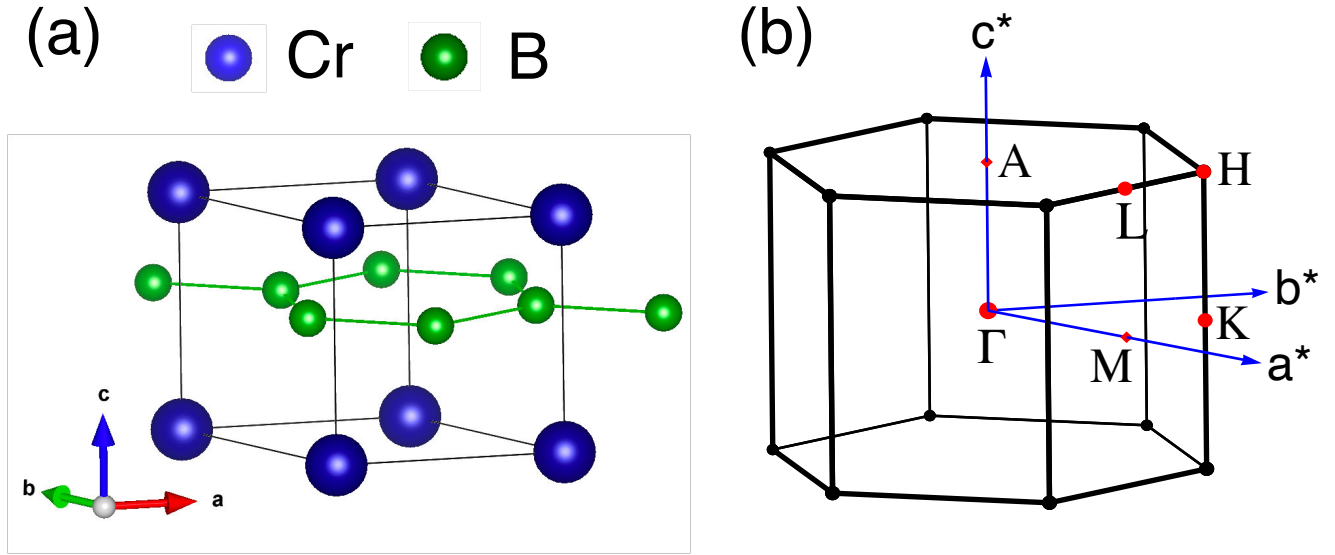


FIG. S2. Crystal structure and BZ of  $\text{CrB}_2$ . It has a  $\text{MgB}_2$ -type structure. The Cr and B atoms form triangular and honeycomb lattices, respectively.

- 
- [1] Yi Liu, Zi-Yi Liu, Jin-Ke Bao, Peng-Tao Yang, Liang-Wen Ji, Ji-Yong Liu, Chen-Chao Xu, Wu-Zhang Yang, Wan-Li Chai, Jia-Yi Lu, Chang-Chao Liu, Bo-Sen Wang, Hao Jiang, Qian Tao, Zhi Ren, Xiao-Feng Xu, Chao Cao, Zhu-An Xu, Jin-Guang Cheng, and Guang-Han Cao, “Superconductivity emerged from density-wave order in a kagome bad metal,” (2023), [arXiv:2309.13514](https://arxiv.org/abs/2309.13514).
- [2] Cuiying Pei, Pengtao Yang, Chunsheng Gong, Qi Wang, Yi Zhao, Lingling Gao, Keyu Chen, Qiangwei Yin, Shangjie Tian, Changhua Li, Weizheng Cao, Hechang Lei, Jinguang Cheng, and Yanpeng Qi, “Pressure-induced superconductivity in itinerant antiferromagnet  $\text{crb}_2$ ,” (2021), [arXiv:2109.15213](https://arxiv.org/abs/2109.15213).